doi:10.1093/brain/awl284 *Brain* (2007), **130**, 394–403

Charcot–Marie–Tooth disease type 2E, a disorder of the cytoskeleton

Gian Maria Fabrizi,[1] Tiziana Cavallaro,[1] Chiara Angiari,[1] Ilaria Cabrini,[1] Federica Taioli,[1] Giovanni Malerba,[2] Laura Bertolasi[1] and Nicolo' Rizzuto[1]

[1]Section of Clinical Neurology, Department of Neurological and Visual Sciences, University of Verona, Italy and [2]Section of Biology and Genetics, Department of Mother and Child and Biology-Genetics, University of Verona, Italy

Correspondence to: Dr Gian Maria Fabrizi, Section of Clinical Neurology, Department of Neurological and Visual Sciences, University of Verona. Policlinico "G.B. Rossi", P.le L.A. Scuro 10, 37134 Verona, Italy
E-mail: gianmaria.fabrizi@univr.it

The neurofilament light chain (NF-L) is a major constituent of intermediate filaments and plays a pivotal function in the assembly and maintenance of axonal cytoskeleton. Mutations in the NF-L gene (NEFL) cause autosomal dominant neuropathies that are classified either as axonal Charcot–Marie–Tooth (CMT) type 2E (CMT2E) or demyelinating CMT type 1F (CMT1F). The pathophysiological bases of the disorder(s) are elusive. We performed a mutational analysis of NEFL in a series of 177 index cases with CMT and without mutations in the genes for peripheral myelin protein zero (MPZ), peripheral myelin protein 22 (PMP22) and connexin 32 (GJB1); the motor nerve conduction velocity (MNCV) at the median nerve was below 38 m/s in 76 cases and above 38 m/s in 101. We identified five new pedigrees with four mutations in the head and rod domains of NF-L, including a novel Leu268Pro substitution and a novel del322Cys_326Asn deletion. Several examined affected members exhibited marked variability in the severity of disease and age at onset. Nerve conduction alterations were consistent with an axonal neuropathy often associated with demyelinating features, such as prolonged distal latencies (DL). Pathological examination of sural nerve biopsies in the probands detected in four cases a chronic axonal neuropathy dominated by focal accumulations of NF with axonal swellings (giant axons) and significant secondary demyelination; in the fifth case no NFs accumulations were evident but many myelinated fibres consisted exclusively of microtubules with few or absent NF. The pathological phenotype correlated with the pattern of nerve conduction alterations and indicated that NEFL mutations cause a profound alteration of the cytoskeleton possibly related to defective targeting of NF.

Keywords: Charcot–Marie–Tooth disease; neurofilament light chain subunit; giant axons; secondary demyelination; phenotype and genotype correlations

Abbreviations: CMT = Charcot–Marie–Tooth; MNCV = motor nerve conduction velocity; NF-L = neurofilament light; SNP = single nucleotide polymorphism

Received June 17, 2006. Revised August 19, 2006. Accepted August 23, 2006. Advance Access publication October 18, 2006.

Introduction

Autosomal dominant Charcot–Marie–Tooth (CMT) disease is classified according to electrophysiological and pathological criteria. CMT type 1 (CMT1) is a de-remyelinating neuropathy manifesting with reduced nerve conduction velocities (NCV); CMT type 2 (CMT2) is an axonal neuropathy with relatively preserved NCV but decreased sensory and compound motor action potentials (SNAP and CMAP). In current practice, the distinction between CMT1 and CMT2 relies simply on the cut-off value of motor nerve conduction velocity (MNCV) at the median nerve (CMT1 <38 m/s; CMT2 >38 m/s) (Reilly, 2005). Separating the demyelinating and axonal forms is challenged by neuropathies that are electrophysiologically and pathologically intermediate between CMT1 and CMT2 and are transmitted with autosomal dominant (dominant intermediate CMT, DI-CMT) or X-dominant inheritance (CMTX). CMT1, CMT2 and DI-CMT are genetically heterogeneous. CMT1 has four genes (CMT1A-D); CMT2 has at least eight loci

(CMT2A-G, CMT2L) with six genes identified; and DI-CMT has three loci and two genes (Zűchner *et al.*, 2005; Jordanova *et al.*, 2006).

New genes and proteins added confusion to the nosography of CMT. For instance, the NEFL gene coding the neurofilament light chain (NF-L) was originally associated with CMT type 2E (CMT2E) (Mersiyanova *et al.*, 2000). Afterwards, because some patients had markedly reduced NCV, the NEFL-related neuropathy was designated as CMT1F (De Jonghe *et al.*, 2001; Jordanova *et al.*, 2003). The pathophysiological bases of such an ambiguous phenotype are elusive. NF-L is the pivotal subunit of NFs, the major intermediate filament (IF) of neurons and axons, and plays a crucial role in the maintenance of the cytoskeleton. Few patients with NEFL mutations have been examined pathologically. One patient with a Glu89Lys mutation had an aspecific axonal neuropathy (Jordanova *et al.*, 2003). Two patients with a Glu396Lys substitution had a mixed axonal and demyelinating neuropathy (Zűchner *et al.*, 2004). A fourth patient with a Pro22Ser mutation had a giant axonal neuropathy (Fabrizi *et al.*, 2004).

Here we reported the identification of five additional pedigrees with four NEFL mutations and described the associated clinical and electrophysiological features. Nerve biopsies in the index cases disclosed a chronic axonal neuropathy caused by derangement of the cytoskeletal architecture with the frequent occurrence of giant axons, axonal atrophy and secondary structural alterations in the myelin sheath. These findings correlated with electroneurographical changes appropriate for an axonal neuropathy having demyelination features, such as prolonged distal latencies (DL). The pathological picture suggested that mutant NF-L subunits altered the formation and maintenance of the cytoskeletal network.

Patients and methods

Patients

A cohort of 177 index Italian patients were referred to our Institution to undergo molecular screening for CMT. NEFL mutations were analysed after excluding mutations in the genes of peripheral myelin protein 22 (PMP22) (CMT1A), myelin protein zero (MPZ) (CMT1B) and connexin 32 (GJB1) (CMTX) as already described (Fabrizi *et al.*, 2004). Of the 177 patients screened, 76 had median MNCV below 38 m/s (age range 7–81 years; 42 males and 34 females), and 101 had median MNCV above 38 m/s (age range 8–81 years; 62 males and 39 females). In 74 patients the family history was consistent with dominant inheritance whereas 103 were apparently isolated with no family history or laboratory findings suggestive of an acquired neuropathy.

Among the five pedigrees with identified mutations, pedigree A has been described elsewhere as a distinct form of CMT characterized pathologically by giant axons and genetically by no linkage to any of the known loci and genes (Lus *et al.*, 2003). Patients from pedigrees B, C, D and E (Fig. 1) were examined clinically and neurophysiologically at our Institution. Muscle strength was graded by the standard Medical Research Council (MRC) scale. The overall impairment was assessed according the CMT neuropathy score, an ad hoc validated scale that takes into account both clinical and neurophysiological measures and distinguishes mild (⩽10), moderate (11–20) and severe (⩾21) disease (Shy *et al.*, 2005).

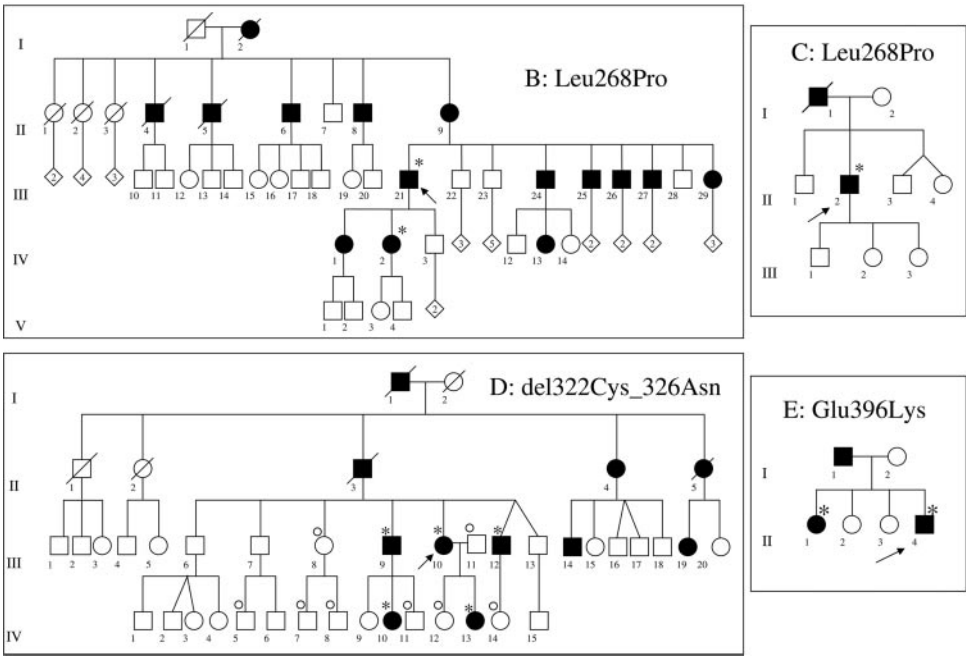

Fig. 1 Pedigrees of families B, C, D and E. The arrows indicate the probands. Square = male, circle = female Solid symbol = affected individuals. An '*' indicates molecularly tested individuals with the mutation; an '°' indicates molecularly tested individuals without the mutation.

Nerve conduction studies and brainstem auditory evoked potentials (BAEP) were performed according to standard methods.

Mutational analysis of NEFL

Genomic DNA was extracted from patients and controls according to standard procedures after obtaining an informed consent. *NEFL* mutations were investigated by denaturing high performance liquid chromatography (DHPLC) using a WAVE® System 1500 device with the Navigator™ Software (*Transgenomic*); the oligonucleotides for PCR and analytical conditions of DHPLC are reported in the Supplementary Table E1.

All PCR fragments containing DHPLC alterations were analysed on both directions by automated nucleotide sequencing using an ALFexpressTM DNA sequencer (*Amersham Pharmacia Biotech*) as done previously (Fabrizi *et al.*, 2004).

The reference cDNA sequence was represented by the GeneBank clone BC039237 (Strausberg *et al.*, 2002). Nucleotide substitutions were numbered relative to the first translated base (the A from the ATG initiation codon).

To investigate whether the detected mutations co-segregated with CMT, the mutational analysis was extended to available affected and unaffected family members (Fig. 1) as well as to 150 healthy Caucasian individuals.

Haplotype tagging single nucleotide polymorphisms and haplotypes frequency of the NEFL gene region

The following single nucleotide polymorphism (SNP) were selected from the HapMap database (http://www.hapmap.org) because they tagged the most common *NEFL* haplotypes in the Caucasian population: rs6998940, rs3757985, rs12545967, rs2976425. SNP were analysed by automated nucleotide sequencing.

The genotyping method was able to detect genotypes of the rs7017329 and rs2976424 SNPs because they are close to rs6998940 and rs2976425, respectively. Therefore, both the SNPs were included in the molecular analysis.

Genotyping was performed in patients III-21 and IV-2 of pedigree B and II-2 of pedigree C and in 50 unrelated Caucasian healthy controls (100 chromosomes).

The SNP rs6998940 showed an absolute linkage disequilibrium with the SNP rs7017329 and thus it was not included in the statistical analysis. Haplotypes frequency was estimated by haplo.em program of library haplo.stats of the statistical software R (http://www.R-project.org).

Histopathology, electron microscopy and morphometry

Archive sural nerve biopsies available for the probands of pedigrees B, C, D and E were processed for histological, ultrastructural and teased-fibre examination as described (Fabrizi *et al.*, 2004). For morphometrical analysis, randomly chosen fields of transverse semithin sections (total area = 0.4 mm^2) were photographed at 40× magnification and analysed with an AxioVision LE 4.2 system (*Zeiss*).

Immunohistochemistry of cytoskeletal components

To assess the expression of NF subunits in axonal swellings, serial paraffin sections were processed by immunocytochemistry using a rabbit polyclonal antibody directed against the monkey light subunit (NF-L) (*Chemicon*, dilution 1:200) and a rabbit polyclonal antibody against the C-terminus of the phosphorylated and non-phosphorylated rat heavy subunit (NF-H) (*Chemicon*, dilution 1:200). Primary antibodies were labelled with swine anti-rabbit immunoglobulins (*DAKO*, dilution 1:100) and revealed with the peroxidase–antiperoxidase (PAP) complex (rabbit PAP, *DAKO*; dilution 1:100) in the presence of 3,3′-diaminobenzidine (DAB) and hydrogen peroxide as chromogen substrate.

To evaluate the co-expression of NF and microtubules by confocal microscopy, cryostatic sections of sural nerves were reacted with rabbit antibodies against NF-L or NF-H (*Chemicon*, dilution 1:200) and a mouse monoclonal antibody against the tubulin β-III isoform (*Chemicon*, 1:50). NF were stained with a fluorescein-conjugate secondary antibody directed against rabbit IgG (Chemicon, 1:100) whereas tubulin was stained with a biotinylated secondary antibody against mouse IgG (*Amersham Pharmacia Biotech*, dilution *1:100*) revealed with Texas Red streptavidin (*Vector laboratories*, dilution 1:100). Sections were analysed using a confocal laser scanning microscope system (*Zeiss*, LSM 510) equipped with an argon 418-λ and a helio-neon 543-λ laser. For double fluorescence, data from two channels were collected simultaneously and analysed in merged images where colocalized tubulin (red) and NF (green) appeared yellow.

Results

NEFL mutations and polymorphisms

Mutational analysis of the *NEFL* coding sequences identified four mutations cosegregating with CMT in five pedigrees (Fig. 1) and several polymorphisms (Table 1). Pedigree A had a c.64C>T nucleotide change causing a Pro22Ser substitution (Supplementary Figure E1); this mutation was already found in CMT2E (Georgiou *et al.*, 2002; Fabrizi *et al.*, 2004) and affected the globular N-terminal head that regulates the protein assembly properties (Omary *et al.*, 2004). The other mutations were all distributed in the central α-helical coil-coiled rod domain which forms the core of NF oligomers. Pedigrees B and C had a novel c.803T > C change leading to a Leu268Pro mutation that perturbed the α-helix of the rod by substituting an aliphatic amino acid with an aliphatic and cyclic residue (Supplementary Figure E1). Pedigree D had a novel deletion of 15 nt (c.963_977delATGCCGGGGCATG-AA) causing an in-frame deletion of 5 amino acids (del322Cys_326Asn) (Supplementary Figure E-2). Pedigree E had a c.1186G > A change leading to a Glu396Lys substitution at the end of the rod (Supplementary Figure E1); the same mutation has already been described in CMT2E though differently recorded as Glu397Lys because of divergences between the reference sequences (Zűchner *et al.*, 2004) (Supplementary Figure E-3).

Haplotypes of the NEFL region

Out of the possible 32 haplotypes we observed six common haplotypes with an estimated frequency above 5% in the 50 control individuals. The most probable haplotype configuration of patients with the Leu268Pro mutation included the haplotype GCCCG (H3 in the electronic

Table 1 Neurofilament light (NEFL) gene mutations and polymorphisms

Nucleotide change	Exon	Amino acid change	Domain	Frequency in CMT index patients	Frequency in normal individuals	Restriction site change	Reference
MUTATIONS							
(pedigree)							
c.64C>T (pedigree A)	1	Pro22Ser	Head	1/177	0/150	+AatII, +FinI, −HgaI, +MaeII, −MwoI	Georgiou *et al.* (2002); Fabrizi *et al.* (2004)
c.803T>C (pedigrees B, C)	1	Leu268Pro	Rod	2/177	0/150	+MspI, +HpaII,−EaeI	—
c.963_977delATGCCGGGGCATGAA (pedigree D)	1	del322Cys_326Asn	Rod	1/177	0/150	−NspI, −PaeI, +Eco47III	—
c.1186G>A (pedigree E)	3	Glu396Lys	Rod	1/177	0/150	—	Choi *et al.* (2004); Züchner *et al.* (2004)
POLYMORPHISMS							
c.45G>A	1	Lys15Lys	Head	0/177	1/150	−Bs1I	—
c.639C>G	1	Ile213Met	Rod	0/177	1/150	—	—
c.667C>T	1	Leu223Leu	Rod	2/177	1/150	Eco57I, −Hpy188I	Jordanova *et al.* (2003)
c.969G>T	1	Arg323Arg	Rod	0/177	1/150	+BstDSI	—
c.1212C>T	3	Ser404Ser	Tail	1/177	1/150	+BsrI, −MwoI, +RleAI, +TspRI	Jordanova *et al.* (2003)
c.1402G>A	3	Asp468Asn	Tail	1/177	0/150	−FokI, −SecI, −StyI	Vechio *et al.*(1996); Jordanova *et al.* (2003)

Restriction endonucleases that may be used to test the presence or absence of mutation are reported (+ = creation and − = abolition of the restriction endonuclease site).
The c.1402G > A change leading to an Asp468Asn substitution occurred in a sporadic patient; this variation was a polymorphism because it affected a phylogenetically nonconserved residue, occurred in normal individuals (Vechio *et al.*, 1996) and had no phenotypical consequences *in vitro* (Perez-Olle *et al.*, 2004). The c.639C > G change leading to a conservative Ile213Met occurred in a healthy control individual and changed a phylogenetically nonconserved residue. Genetic variations included four SNP not recorded in the electronic databases (http://www.ncbi.nlm.nih.gov/projects/SNP). None of the detected polymorphisms occurred in the molecularly tested patients from pedigrees A–E.

Table 2 Clinical features of the examined patients

Pedigree (mutation) case/sex/years	CMTNS	Onset (decade)	Wasting/weakness		Loss of touch sense		Loss of vibration sense		Reflexes (prox/dist)	Additional features
			LL	UL	LL	UL	LL	UL		
Pedigree B (Leu268Pro)										
III-21/M/59	Moderate	2nd	++/++	++/+	+	−	+++	++	D/A	Hearing loss
III-24/M/51	Mild	2nd	++/+	+/−	−	−	+	−	D/D	—
IV-2/F/30	n.c.	1st	+/+	−/−	−	−	−	−	D/D	—
IV-13/F/21	Mild	1st	+/−	−/−	−	−	−	−	D/D	—
Pedigree C (Leu268Pro)										
II-2/M/50	Moderate	5th	+++/++	+/−	+	−	++	++	A/A	Hearing loss
Pedigree D (del322Cys_326Asn)										
III-9/M/49	Moderate	1st	+++/+++	+++/++	−	−	+++	−	D/A	Sensory ataxia, postural tremor
III-10/F/47	Moderate	1st	+/++	−/−	+	+	+++	−	N/A	Sensory ataxia
III-12/M/46	Moderate	1st	+++/++	++/+	−	−	+	−	D/A	Hearing loss, postural tremor
IV-10/F/20	Mild	1st	+/+	+/+	−	−	+	−	D/A	Episodic ataxia, postural tremor
IV-13/F/21	Mild	1st	++/+	+/−	−	−	−	−	N/A	Episodic ataxia
Pedigree E (Glu396Lys)										
II-1/F/46	Moderate	1st	+++/+++	++/−	−	−	+++	++	A/A	Hearing loss
II-4/M/30	Moderate	2nd	+++/++	+++/++	−	−	+++	+++	A/A	—

M = male; F = female; CMTNS: n.c. = not computable; LL = lower limbs; UL = upper limbs. Wasting of distal muscles: + = mild; ++ = moderate; +++ = severe; − = absent. Weakness of distal muscles: ++++ = MRC 0; +++ = MRC 1–2; ++ = MRC 3; + = MRC 4; − = MRC 5, no weakness. Distal loss of touch and vibration sense: +++ = severe; ++ = moderate; + = mild; − = normal sense. Proximal (prox)/distal (dist) reflexes: N = normal; D = decreased; A = absent.

Table 2) showing an estimated frequency of 10% in healthy controls. Therefore, it is likely that the recurrent Leu268Pro mutation was located on haplotype H3 (shared by the affected individuals) supporting the hypothesis of a founder effect. However, we cannot exclude that it originated independently in pedigrees B and C.

Clinical findings

Pedigree A with the Pro22Ser mutation has been described elsewhere (Lus *et al.*, 2003). Clinical findings of pedigrees B–E are reported in Table 2. Notable features were as follows. The proband II-2 from pedigree C, a 50-year-old policeman, manifested progressive disturbances of gait starting from age 48 years; when 45-year-old, he had undergone a 14 month course of antitubercular treatment with isoniazid, rifampin, ethambutol associated with a full-dose supplementation of pyridoxine; his father had died at 72 years of lung cancer and since 65 years of age he had worn an ankle-foot orthosis because of bilateral foot-drop. The proband III-10 of pedigree D, a 47-year-old female worker had prominent ataxia with a positive Romberg's test and without dysarthria or dysmetria. Because of marked sensory involvement, she had undergone molecular tests to rule out spinocerebellar ataxia 1, 2, 3 and 6. Pedigree D members III-9, III-10, IV-10 and IV-13 reported recurrent episodes of gait and limb unsteadiness associated with feverish illnesses in childhood.

MRI of brain and cervical spinal cord obtained from patients III-9, III-10 and III-12 of pedigree D as well as from patient II-4 of pedigree E, failed to disclose any abnormality.

Neurophysiological findings

Pedigree A was reported previously (Lus *et al.*, 2003). Results of nerve conduction studies in pedigrees B through E are summarized in Table 3. MNCVs in the median nerve ranged from 29.2 m/s with a compound muscle action potential (CMAP) of 2.2 mV to 55.4 m/s with a CMAP of 8.7 mV; in the ulnar nerve MNCV varied from 25.3 m/s with a CMAP of 2.7 mV to 56.2 with a CMAP of 5.6 mV. In some patients (pedigree B, patient IV-13 and pedigree C, patient II-2) the distal motor latencies were disproportionately prolonged compared with conduction slowing in the intermediate nerve segments.

BAEP were obtained in nine patients and were abnormal in all cases except in patient IV-10 of pedigree D (Table 4). Four patients had no potentials (pedigree B, III-21; pedigree C, II-2; pedigree D, III-12; pedigree E, II-1), two had delayed W I-III interpeak latencies (pedigree D, III-9, IV-13), one had a delayed W I-V interpeak latency with normal W I and W I-III latency (pedigree D, III-10); and another patient had delayed W I-V interpeak latency with normal W I latency and an undetectable W I-III (pedigree E, II-4).

Table 3 Results of electroneurography

Pedigree	Median nerve				Ulnar nerve				Peroneal nerve				Sural nerve	
Case/sex/years	MNCV (50–60)	CMAP (>6)	DL (<3.5–4)	F (<29)	MNCV (52–62)	CMAP (>10)	DL (<2.6–3.6)	F (<29)	MNCV (44–52)	CMAP (>6)	DL (<4.5–5.5)	F (<50)	SNCV (44–50)	SNAP (10–12)
Pedigree B														
III-21/M/59	43.5	3.2	5	33	45.8	5.3	4.6	33	—	n.e.	—	—	—	n.e.
III-24/M/51	38	3.4	7.1	n.p.	34.5	4.8	5.25	n.p.	—	n.e.	—	—	—	n.e.
IV-2/F/30		n.p.				n.p.			34.8	2.5	4	n.p.	—	n.e.
IV-13/F/21	55.4	8.7	6.7	n.p.	56.2	5.6	8.3	n.p.	36.6	2	11.7	n.p.	—	n.e.
Pedigree C														
II-2/M/50	48	7	5.4	33	45	7	5.5	35	—	n.e.	—	—	—	n.e.
Pedigree D														
III-9/M/49	39.4	6.9	5.2	40.6	37	1.7	4.1	38.9	—	n.e.	—	—	—	n.e.
III-10/F/47	39.6	14.2	3.5	35.0	37.3	7.2	2.9	38	35.2	1.5	4	n.e.	20	1.1
III-12/M/46	42.4	10.6	3.6	36.7	38	1.8	2.6	37.3	32.3	3	7.6	n.e.	33.3	1.9
IV-10/F/20	44.4	17.2	3.2	38.2	41.4	15.8	2.6	39.5	34.8	4.3	3.8	n.e.	42.9	8.7
IV-13/F/21	46.2	8.5	3.2	41.3	42.9	10.7	2.2	36.5	34.5	9.1	5.9	63	33.3	4
Pedigree E														
II-1/F/46	29.2	2.2	8.9	46	25.3	2.7	3.7	n.e.	—	n.e.	—	—	—	n.e.
II-4 /M/30	30	2.1	7.3	n.e.	35.1	1.1	3.5	n.e.	24.6	0.1	11.3	ne	23.4	2.4

M = male; F = female; MNCV= motor nerve conduction velocity (m/s); CMAP= compound motor action potential (mV); DL= distal motor latency (ms); F = F-wave latency (ms); SNCV= sensory nerve conduction velocity (m/s); SNAP= sensory nerve action potential (μV); n.e. = not evoked; n.p. = not performed. Normal values are reported in parenthesis.

Table 4 Results of BAEP

Case/sex/years	BAEP right/left		
	W I (ms) (<1.7)	W I–III (ms) (<2.3)	W I–V (ms) (<4.3)
Pedigree B			
III-21/M/59	n.e./n.e.	—	—
Pedigree C			
II-2/M/50	n.e./n.e.	—	—
Pedigree D			
III-9/M/49	1.7/1.6	2.6/2.4	4.0/4.1
III-10/F/47	1.5/1.6	2.3/2.2	5.0/4.9
III-12/M/46	n.e./1.5	—	—
IV-10/F/20	1.6/1.6	1.7/2.2	3.8/4.2
IV-13/F/21	1.6/1.6	2.5/2.8	4.8/4.8
Pedigree E			
II-1/F/46	n.e./n.e.	—	—
II-4/M/30	1.8/1.7	—	4.5/4.8

WI= wave-I latency; WI-III = wave I-III interpeak latency; WI-V= wave I-V interpeak latency; n.e. = not evoked. Normal values are reported in parenthesis.

Neuropathological findings

Histograms disclosed a marked reduction in the large diameter-fibres with loss of the bimodal spectrum in all the index cases examined; percentages of myelinated fibres with diameters above 6.0 μm were 17% (pedigree B), 22% (pedigree C), 36% (pedigree D) and 18% (pedigree E). The fibre densities varied markedly (range in 4 age-matched controls = 6300–7100/mm^2 of fascicular area): 1682/mm^2 (pedigree B), 5649/mm^2 (pedigree C), 6153/mm^2 (pedigree D) and 8514/mm^2 (pedigree E). All specimens contained numerous small and mid-size irregular-shaped fibres, some fibre groups resembling regenerating clusters and few fibres encircled by simple onion-bulb structures.

The probands in pedigrees A (Lus *et al.*, 2003), B, C and D disclosed giant axons i.e. axonal swellings surrounded by an extremely thin myelin sheath. Giant axons varied in number and size between different patients being prominent in the probands of pedigrees B and C (Fig. 2). On teased fibres focal swellings were distributed prevalently in the paranodes alternating with segments of reduced calibre; focal swellings had a pale, extremely thin or absent myelin sheath (Fig. 3). At the ultrastructural level the giant axons contained accumulations of regularly [Fig. 4 (I)] or irregularly oriented NF sometimes displaying segregated organelles and microtubules [Fig. 4 (II)]; occasionally, the NF islets were interspersed with accumulations of mitochondria, lysosomes and membranous bodies [Fig. 4 (III)]. Similar NF accumulations were also evident in fibres, which did not appear as giant axons at the histological level. At immunohistochemistry the giant axons had a homogeneous and intense pattern of NF-L and NF-H expression (electronic Fig. 4).

In the proband II-4 of pedigree E, no NF accumulations were detectable. The axoplasm of several fibres had no NF and contained microtubules alone. These fibres displayed structural changes in the myelin sheath, such as loosening of the lamellae and honeycomb-like demyelination [Fig. 4 (IV)]. Confocal immunomicroscopy demonstrated that in this case the expression of tubulin was markedly higher than NF-L when compared with patients with giant axons (electronic Fig. 5).

Discussion

Our study extends the phenotypical variability in CMT linked to *NEFL* mutations and provides clues to its pathogenesis.

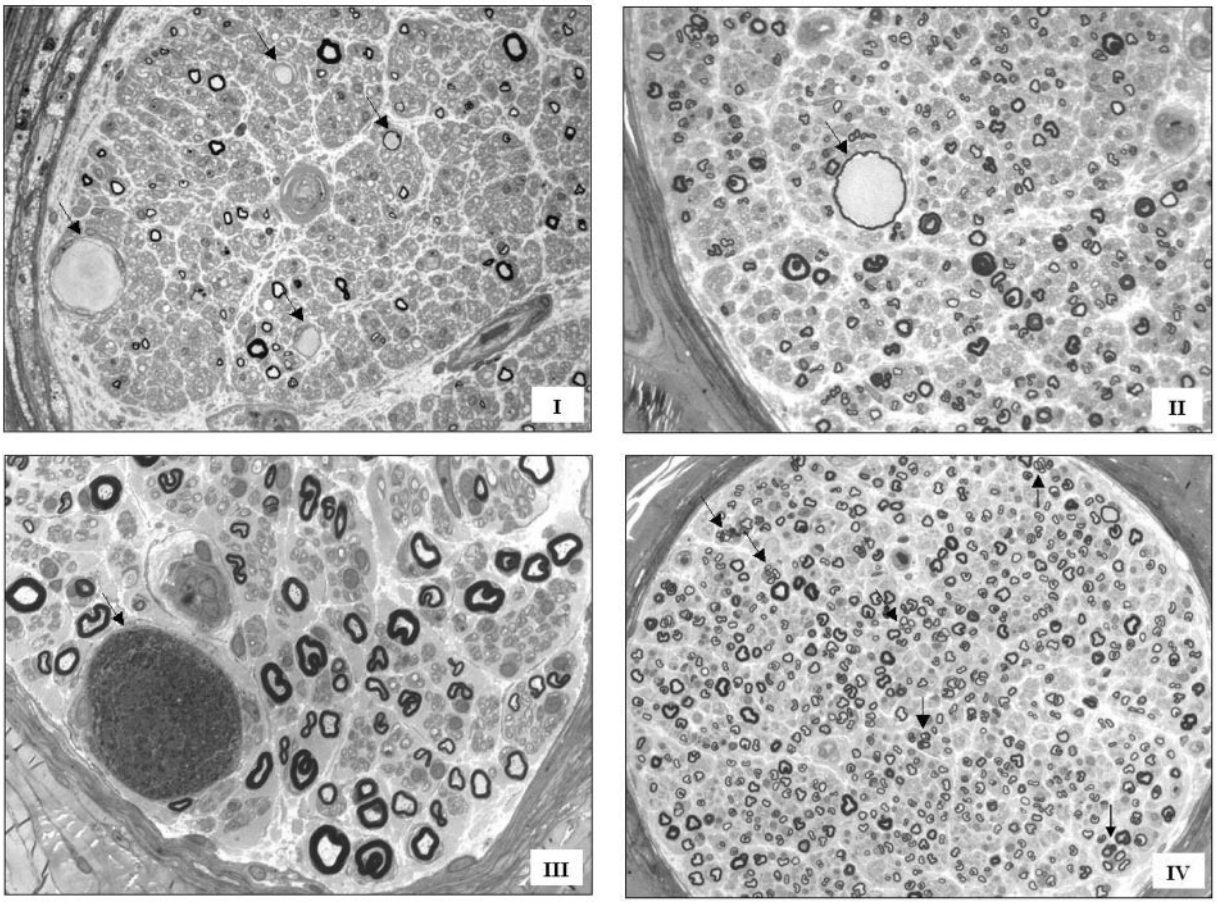

Fig. 2 Semithin sections of sural nerves from the probands of pedigree B (I), C (II), D (III) and E (IV). Original magnification: I and II = 40×; III = 100×; IV = 20×. I and II: loss of large myelinated fibres and axonal swellings (arrows) are evident in the probands of pedigrees B and C harbouring a Leu268Pro mutation. III: a large degenerating axonal swelling (arrow) in pedigree D with the del322Cys-326Asn mutation (see Fig. 4, III for ultrastructural details). IV: many regenerating clusters (arrows) in pedigree E with Glu396Lys.

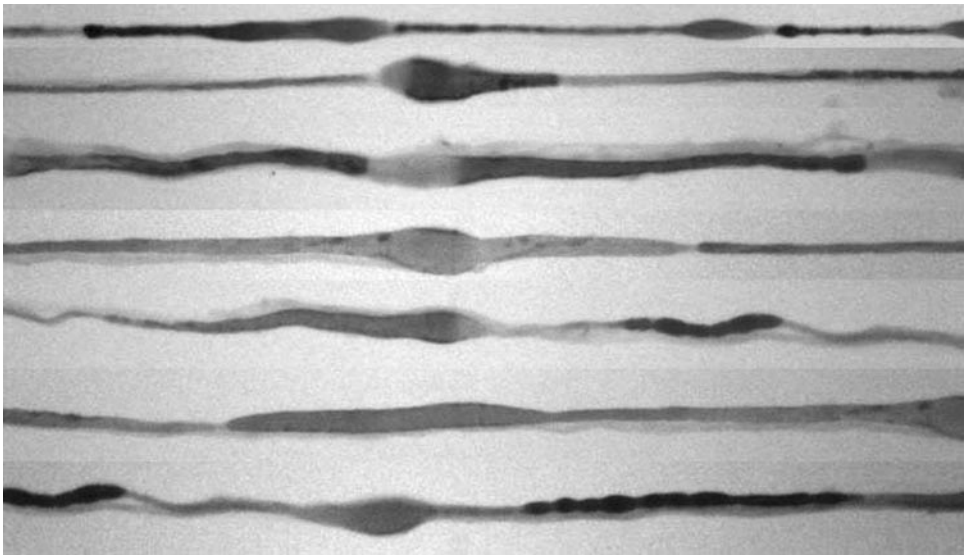

Fig. 3 Teased fibres from the proband of pedigree C. Original magnification: 20×. Axonal swellings are distributed along the fibres alternating with remyelinated or demyelinated segments. Some fibres showed myelin wrinkling as expression of secondary demyelination.

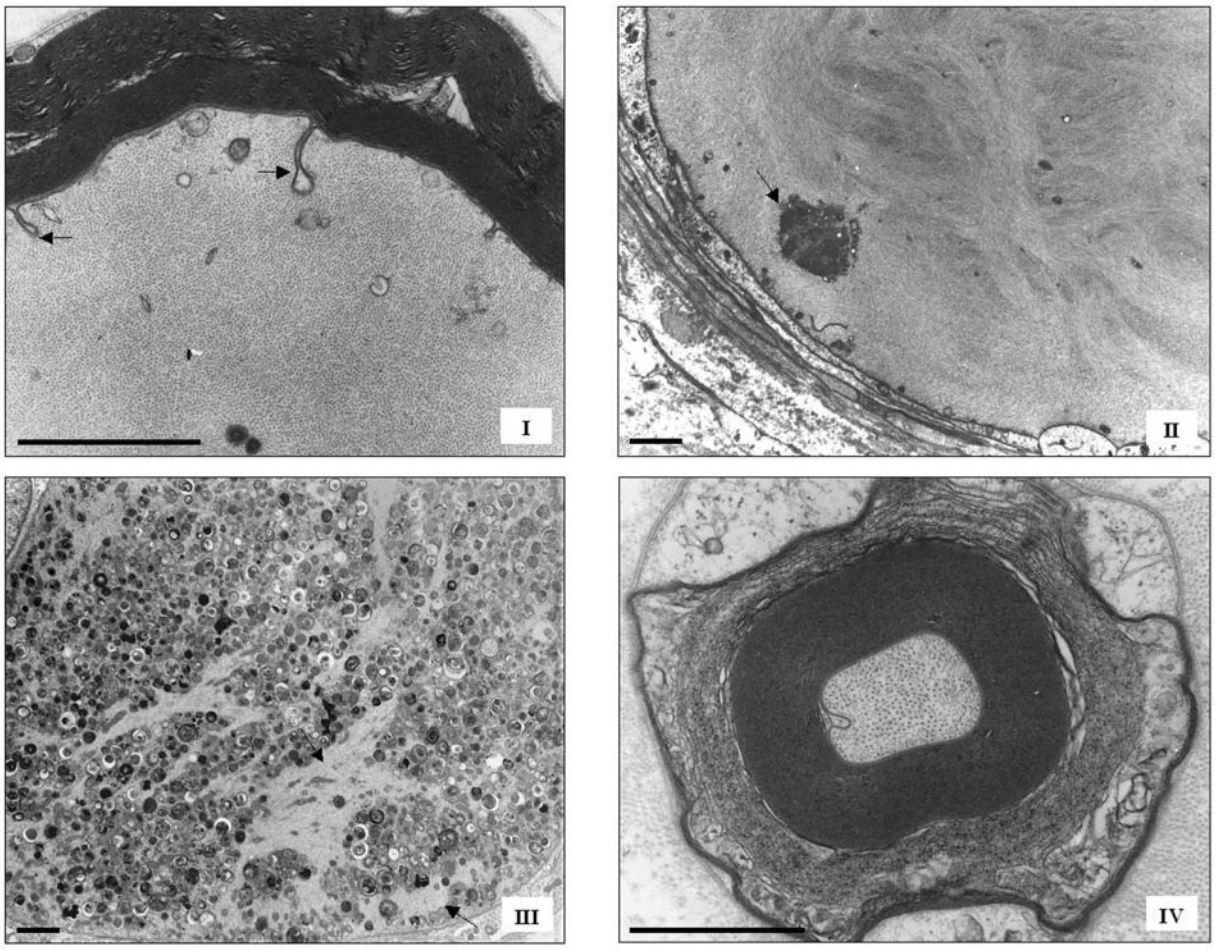

Fig. 4 Electron microscopy of sural nerves from the probands of pedigrees C (I), B (II), D (III) and E (IV) (scaling Bar 2 μm). I: giant axon with regularly oriented NF and introflexion of the myelin sheath (arrows). II: giant axon with a cluster of organelles (arrow) and irregular whorls of NF. III: giant axon (see Fig. 2, III) made up of degenerating organelles and small NF islets (arrows). IV: a fibre whose axoplasm consists almost exclusively of microtubules; note the loosening of external myelin lamellae.

Whereas previous series suggested that CMT2E has early onset and severe evolution (Jordanova *et al.*, 2003) the patients we describe had mild-to-moderate impairment with onset ranging from the first to the fifth decade. *NEFL* mutations therefore seem to cause broadly ranging neuropathies that vary in severity. Several patients had neurosensorial hearing loss or abnormal BAEPs. Because acoustic pathways are clinically or subclinically involved in various hereditary motor and sensory neuropathies, hearing loss is not specific of CMT2E. The family with the 322Cys-326Asn in-frame deletion had prominent sensory involvement and episodic ataxia in childhood triggered by feverishness, similarly to a pedigree with a Glu396Lys substitution described elsewhere (Zűchner *et al.*, 2004). Hence we consider that these peculiar features as well should be encompassed in *NEFL* mutation phenotypical variability.

In the patients studied, nerve conduction changes were distributed predominantly in the lower limbs and were consistent with a mixed, axonal and demyelinating, neuropathy. Median MNCV varied from 29.2 to 55.4 m/s with most patients having values >38 m/s, appropriate for an axonal neuropathy. The only two patients with MNCV <38 m/s (pedigree E) had consensually reduced CMAP, resembling previous findings in the affected members of pedigree A (Lus *et al.*, 2003). This combined reduction of CMAP and MNCV may simply reflect the loss of large-diameter myelinated fibres. In the upper and lower limbs of several patients the DL were nevertheless prolonged disproportionally to the MNCV slowing indicating distal demyelination as seen in hereditary neuropathy with liability to pressure palsies and neuropathy associated with monoclonal IgM antibodies directed against myelin-associated glycoprotein (Kaku *et al.*, 1994; Andersson *et al.*, 2000).

A distinctive finding in this study was the *NEFL*-related pathological process, which provided clues to the nerve conduction changes showing an axonopathy with profound structural alterations in the cytoskeleton and significant secondary demyelination. The pathological phenotype we described here overlapped with the nerve picture found in autosomal recessive Giant Axonal Neuropathy (GAN) caused

by mutations of the cytoskeletal protein gigaxonin, which lead to a generalized disorder of IF organization (Allen *et al.*, 2005). In four out of five newly identified patients (pedigrees A–D), corroborating what we found in our previous CMT2E case (Fabrizi *et al.*, 2004), the pathologic process was dominated by focal accumulations of disorganized NF that appeared as giant axons with a retracted and altered myelin sheath. The number of giant axons varied in different cases and was highest in the nerve biopsies with the Leu268Pro mutation in the rod. The singleton patient without evidence of NF accumulations, the proband in pedigree E, had a Glu396Lys mutation like other two cases with the same mutation described elsewhere in whom no giant axons were reported (Zuchner *et al.*, 2004). Notwithstanding the absence of detectable NF accumulations, the nerve biopsy demonstrated also in that patient profound structural alterations in the cytoskeleton, which often was constituted exclusively by microtubules, accompanied by ultrastructural features of demyelination.

A suitable model for understanding the pathological and electrophysiological correlations in CMT2E is that of human and experimental toxic neuropathies induced by γ-diketones. By cross-linking covalently NF, these toxicants affect NF transport and cause a distal axonopathy marked by NF-filled swellings proximal to the nodes of Ranvier with retraction of the myelin sheath from the node and segmental demyelination (Graham, 1999). In polineuropathies induced by poisoning with n-hexane this pathological process results in low CMAP, prolonged DL and a significant reduction in MNCV mainly affecting the distal limbs segments (Öge *et al.*, 1994). In experimental neuropathies, the spatial distribution of giant axons correlated with the rate of cross-linking by the single drugs: with more potent agents, NF accumulated intraspinally and in proximal ventral roots, whereas with less potent agents they mainly accumulated distally (Graham, 1999).

Additional clues to the pathogenesis of CMT2E came from transfection of some disease-associated NEFL mutants into non-neuronal and neuronal cell cultures. The mutants tested disrupted to various extents NF assembly and the formation of IF networks and perturbed anterograde and retrograde axonal transport (Brownlees *et al.*, 2002; Perez-Olle *et al.*, 2004, 2005). *NEFL* mutants showed defective targeting of NF-L in neuronal catecholaminergic cells; some mutations accumulated proximally, in the cell body, axonal hillock and initial segment of neuritis, whereas other mutations accumulated mainly distally causing focal swellings of the neuritic process (Perez-Olle *et al.*, 2004, 2005). Particularly, also the Pro22Ser mutation reported here was able to disrupt NF assembly and transport leading to NF-L accumulations that recalled those observed in CMT2E (Perez-Olle *et al.*, 2005). The various degrees of toxic potential proper of different mutants (Perez-Olle *et al.*, 2004, 2005) may explain the variability in the number of giant axons that we detected through the distal window of the sural nerve. An exclusively proximal location of the swellings may also explain why no giant axons were detectable in patients with the Glu396Lys mutation and why several axons were devoid of NF and contained microtubules alone.

All CMT2E-associated mutations of NEFL were located in the head and rod domains and were missense with the exception of the del322Cys-326Asn described here and of a Thr21frame-shift (Thr21fs) (Leung *et al.*, 2006). Del322Cys-326Asn did not cause a frameshift in the open reading frame so that it was predicted to lead to a protein that lacked five residues in the central rod. In contrast, Thr21fs in the head domain was a null mutation expected to trigger the nonsense-mediated decay of messenger RNA. When expressed in cell systems, Thr21fs was nevertheless able to disrupt the assembly of the wild-type NF-L and of other IFs, suggesting a toxic gain of function by the truncated head domain (Leung *et al.*, 2006). Conversely, a nonsense out-of-frame mutation that introduced a premature stop codon in the tail domain of NF-L did not co-segregate fully with CMT2E suggesting that haploinsufficiency is not pathogenic or, alternatively, that the tail domain does not play a crucial role (Andrigo *et al.*, 2005). Systematic experimental investigations into various mutants could help to solve the genetical mechanisms responsible for NEFL molecular lesions.

Supplementary material

Supplementary data are available at *Brain* Online.

Acknowledgements

The authors gratefully acknowledge the families for participating in this study. The authors thank Prof. Antonino Uncini for critical reading of the manuscript, Dr Maria Pellegrini for preparing the tables, Prof. Salvatore Monaco, Dr Ettore Nardelli and Dr Daniele Orrico for referring the patients. The work was supported by MIUR (grant no. 2005060584 to N.R.), Fondazione Mariani (grant 2005–2007 to N.R.), Telethon-Italy (grant no. GUP04009 to G.M.F.) and Fondazione CariVerona (grant 2005–2007 to N.R.). Funding to pay the Open Access publication charges for this article was provided by MIUR and Fondazione Mariani.

References

Allen E, Ding J, Wang W, Pramanik S, Chou J, Yau V, et al. Gigaxonin-controlled degradation of MAP1B light chain is critical to neuronal survival. Nature 2005; 438: 224–8.

Andersson PB, Yen E, Parko K, So YT. Electrodiagnostic features of hereditary neuropathy with liability to pressure palsies. Neurology 2000; 54: 40–4.

Andrigo C, Boito C, Prandini P, Mostacciuolo ML, Siciliano G, Angelici C, et al. A novel out-of-frame mutation in the neurofilament light chain gene (NEFL) does not result in Charcot–Marie–Tooth disease type 2E. Neurogenetics 2005; 6: 49–50.

Brownlees J, Ackerley S, Grierson AJ, Jacobsen NJ, Shea K, Anderton BH, et al. Charcot–Marie–Tooth disease neurofilament mutations disrupt neurofilament assembly and axonal transport. Hum Mol Genet 2002; 11: 2837–44.

Choi BO, Lee MS, Shin SH, Hwang JH, Choi KG, Kim WK, et al. Mutational analysis of PMP22, MPZ, GJB1, EGR2 and NEFL in Korean Charcot–Marie–Tooth neuropathy patients. Hum Mutat 2004; 24: 185–6.

De Jonghe P, Mersiyanova I, Nelis E, Del Favero J, Martin JJ, Van Broeckhoven C, et al. Further evidence that neurofilament light chain gene mutations can cause Charcot–Marie–Tooth disease type 2E. Ann Neurol 2001; 49: 245–9.

Fabrizi GM, Cavallaro T, Angiari C, Bertolasi L, Cabrini I, Ferrarini M, et al. Giant axons and neurofilament accumulation in Charcot–Marie–Tooth disease type 2E. Neurology 2004; 62: 1429–31.

Georgiou DM, Zidar J, Korosec M, Middleton LT, Kyriakides T, Christodoulou K. A novel NF-L mutation Pro22Ser is associated with CMT2 in a large Slovenian family. Neurogenetics 2002; 4: 93–6.

Graham DG. Neurotoxicants and the cytoskeleton. Curr Opin Neurol 1999; 12: 733–7.

Jordanova A, De Jonghe P, Boerkel CF, Takashima SH E, De Vriendt E, Ceuterick C, et al. Mutations in the neurofilament light chain gene (NEFL) cause early onset severe Charcot–Marie–Tooth disease. Brain 2003; 126: 590–7.

Jordanova A, Irobi J, Thomas FP, Van Dijk P, Meerschaert K, Dewil M, et al. Disrupted function and axonal distribution of mutant tyrosyl-tRNA synthetase in dominant intermediate Charcot–Marie–Tooth neuropathy. Nat Genet 2006; 38: 197–202.

Kaku DA, England JD, Sumner AJ. Distal accentuation of conduction slowing in polyneuropathy associated with antibodies to myelin-associated glycoprotein and sulphated glucuronyl paragloboside. Brain 1994; 17: 941–7.

Leung CL, Nagan N, Graham TH, Liem RK. A novel duplication/insertion mutation of NEFL in a patient with Charcot–Marie–Tooth disease. Am J Med Genet A 2006; 140: 1021–5.

Lus G, Nelis E, Jordanova A, Lofgren A, Cavallaro T, Ammendola A, et al. Charcot–Marie–Tooth disease with giant axons: a clinicopathological and genetic entity. Neurology 2003; 61: 988–90.

Mersiyanova IV, Perepelov AV, Polyakov AV, Sitnikov VF, Dadali EL, Oparin RB, et al. A new variant of Charcot–Marie–Tooth disease type 2 is probably the result of a mutation in the neurofilament-light gene. Am J Hum Genet 2000; 67: 37–46.

Öge AM, Yazici J, Boyaciyan A, Eryildiz D, Ornek I, Konyalioglu R, et al. Peripheral and central conduction in n-hexane polyneuropathy. Muscle Nerve 1994; 17: 1416–30.

Omary MB, Coulombe PA, McLean WH. Intermediate filament proteins and their associated diseases. N Engl J Med 2004; 351: 2087–100.

Perez-Olle R, Jones ST, Liem RK. Phenotypic analysis of neurofilaments light gene mutations linked to Charcot–Marie–Tooth disease in cell culture models. Hum Mol Genet 2004; 13: 2207–20.

Perez-Olle R, Lopez-Toledano MA, Goryunov D, Cabrera-Poch N, Stefanis L, Brown K, et al. Mutations in the neurofilament light gene linked to Charcot–Marie–Tooth disease cause defects in transport. J Neurochem 2005; 93: 861–74.

Reilly MM. Axonal Charcot–Marie–Tooth disease. The fog is slowly lifting. Neurology 2005; 65: 186–7.

Shy ME, Blake J, Krajewski K, Fuerst DR, Laura M, Hahn AF, et al. Reliability and validity of the CMT neuropathy score as a measure of disability. Neurology 2005; 64: 1209–14.

Strausberg RL, Feingold EA, Grouse LH, Derge JG, Klausner RD, Collins FS, et al. Generation and initial analysis of more than 15,000 full-length human and mouse cDNA sequences. Proc Natl Acad Sci USA 2002; 99: 16899–903.

Vechio JD, Bruijn LI, Xu Z, Brown RH, Cleveland DW. Sequence variants in human neurofilament proteins: absence of linkage to familial amyotrophic lateral sclerosis. Ann Neurol 1996; 40: 603–10.

Zűchner S, Vorgerd M, Sindern E, Schrőder JM. The novel neurofilament light (NEFL) mutation Glu397Lys is associated with a clinically and morphologically heterogeneous type of Charcot–Marie–Tooth neuropathy. Neuromuscul Disord 2004; 14: 147–57.

Zűchner S, Noureddine M, Kennerson M, Verhoeven K, Claeys K, De Jonghe P, et al. Mutations in the pleckstrin homology domain of dynamin 2 cause dominant intermediate Charcot–Marie–Tooth disease. Nat Genet 2005; 37: 289–94.